Neuron, Vol. 20, 495–508, March, 1998, Copyright ©1998 by Cell Press

Expression of a Protein Kinase C Inhibitor in Purkinje Cells Blocks Cerebellar LTD and Adaptation of the Vestibulo-Ocular Reflex

Chris I. De Zeeuw,*§ Christian Hansel,†§ Feng Bian,‡ Sebastiaan K.E. Koekkoek,* Adriaan M. van Alphen,* David J. Linden,† and John Oberdick‡‖
*Department of Anatomy
Erasmus University Rotterdam
3000 DR Rotterdam
The Netherlands
†Department of Neuroscience
The Johns Hopkins University School of Medicine
Baltimore, Maryland 21205
‡Department of Cell Biology
Neurobiology and Anatomy/Neuroscience Division
and the Neurobiotechnology Center
The Ohio State University
Columbus, Ohio 43210

Summary

Cerebellar long-term depression (LTD) is a model system for neuronal information storage that has an absolute requirement for activation of protein kinase C (PKC). It has been claimed to underlie several forms of cerebellar motor learning. Previous studies using various knockout mice (mGluR1, GluRδ2, glial fibrillary acidic protein) have supported this claim; however, this work has suffered from the limitations that the knockout technique lacks anatomical specificity and that functional compensation can occur via similar gene family members. To overcome these limitations, a transgenic mouse (called L7-PKCI) has been produced in which the pseudosubstrate PKC inhibitor, PKC[19–31], was selectively expressed in Purkinje cells under the control of the *pcp-2(L7)* gene promoter. Cultured Purkinje cells prepared from heterozygous or homozygous L7-PKCI embryos showed a complete blockade of LTD induction. In addition, the compensatory eye movements of L7-PKCI mice were recorded during vestibular and visual stimulation. Whereas the absolute gain, phase, and latency values of the vestibulo-ocular reflex and optokinetic reflex of the L7-PKCI mice were normal, their ability to adapt their vestibulo-ocular reflex gain during visuo-vestibular training was absent. These data strongly support the hypothesis that activation of PKC in the Purkinje cell is necessary for cerebellar LTD induction, and that cerebellar LTD is required for a particular form of motor learning, adaptation of the vestibulo-ocular reflex.

Introduction

In recent years, there has been considerable interest in electrophysiological model systems of information storage in the brain such as long-term potentiation (LTP) and long-term depression (LTD). These phenomena have been proposed as candidate mechanisms to underlie memory storage in the behaving animal because they have attractive computational properties including their duration, input specificity, and associativity (reviewed by Linden and Connor, 1995) and because they have been manifest in regions of the brain that appear to be necessary for certain forms of behavioral learning as assessed with lesion and drug infusion studies. For example, the hippocampus, where LTP and LTD have been most extensively investigated, is necessary for certain forms of spatial learning, and the cerebellum, where a different form of LTD has been studied, is necessary for certain forms of motor learning such as associative eyeblink conditioning and adaptation of the vestibulo-ocular reflex (VOR). Unfortunately, testing the hypothesis that LTP and LTD in particular brain regions underlie specific behavioral phenomena has been a difficult endeavor.

The advent of transgenic mouse technology, in particular the use of embryonic stem cells and homologous recombination "knockout" methods, has made it possible to test the role of various signaling molecules in LTP and LTD together with behavioral analysis of the appropriate learning tasks (reviewed by Chen and Tonegawa, 1997). However, there have been three major problems that have complicated the analysis of knockout mice. First, knockout mice have the gene of interest deleted from the earliest stages of development. As a result, these mice often have a complex developmental phenotype. For example, PKCγ, mGluR1, and GluRδ2 knockout mice all have cerebellar Purkinje cells that fail to undergo the normal developmental conversion from multiple to mono climbing fiber innervation in early postnatal life (Chen et al., 1995; Kano et al., 1995, 1997; Kashiwabuchi et al., 1995). Second, knockout of one gene sometimes produces compensatory upregulation in the expression of other related genes during development. In the CREBα-δ knockout mouse, there is compensatory upregulation of the related transcription factor CREM (Hummler et al., 1994; Blendy et al., 1996). Similarly, it has been suggested that PKCγ knockout mice do not show impaired cerebellar motor learning due to compensation by other PKC isoforms in Purkinje cells (Chen et al., 1995). A third complicating factor is that knockout mice have the gene of interest deleted in every cell of the body, not just the cells of interest, making it more difficult to ascribe the knockout's behavioral effects to dysfunction in any one particular structure or cell type. This is a potential problem for the analysis of behaviors that are likely to require use-dependent plasticity at multiple sites. For example, associative eyeblink conditioning and VOR adaptation have been suggested to require plasticity at parallel fiber Purkinje cells and the synapses made by Purkinje cell axons en route to their targets in the deep cerebellar or vestibular nuclei (Yeo et al., 1985; Khater et al., 1993; Pastor et al., 1994; Raymond et al., 1996; Highstein et al., 1997).

To address the latter two complications, we have taken a different approach. Cerebellar LTD is an attenuation of the parallel fiber-Purkinje cell synapse that occurs

§ These authors contributed equally to this work.
‖ To whom correspondence should be addressed.

when parallel fiber and climbing fiber inputs to a Purkinje cell are coactivated at moderate frequencies (Ito et al., 1982; Linden and Connor, 1995). It has been suggested to underlie several forms of motor learning, including adaptation of the VOR, associative eyeblink conditioning, and limb load adjustment (Ito, 1982, 1989; Thompson and Krupa, 1994; Raymond et al., 1996; but see Llinás et al., 1997). The induction of cerebellar LTD may be blocked by internal application of PKC inhibitors in Purkinje cells (Linden and Connor, 1991; Narasimhan and Linden, 1996). Thus, if cerebellar LTD is necessary for these particular forms of motor learning, then inhibition of PKC in cerebellar Purkinje cells would be expected to interfere specifically with them. Using the promoter of the Purkinje cell-specific gene *pcp-2(L7)* (Oberdick et al., 1990), transgenic mice have been created in which a selective inhibitor to a broad range of PKC isoforms is chronically overexpressed (House and Kemp, 1987; Linden and Connor, 1991). This strategy ensures that in L7-PKCI mice, PKC inhibition will be restricted to Purkinje cells, and that compensation via upregulation of different PKC isoforms will not succeed in blunting the biochemical effect of the transgene. We have subjected these mice to biochemical, anatomical, electrophysiological, and behavioral analysis to test the hypotheses that PKC activation is required for LTD induction and that LTD induction is required for adaptation of the vestibulo-ocular reflex.

Results

Construction of L7-PKCI Mice

A minigene (PKCI) was made by hybridization of two complementary synthetic oligonucleotides, each 50 bases in length, producing a double-stranded product with 5′ overhangs compatible with BamHI restriction sites (see Experimental Procedures). This fragment was cloned into the BamHI site of the Purkinje cell expression vector, L7ΔAUG (Smeyne et al., 1995), in which all possible translational initiation sites were removed (Figure 1A). The minigene, if expressed, would encode a 13 amino acid peptide (not including the start methionine) corresponding in sequence to PKC[19–31] (Figure 1B), a slightly truncated version of the pseudosubstrate domain of PKC, PKC[19–36] (House and Kemp, 1987; Linden and Connor, 1991). This version has been demonstrated in vitro to be a more potent inhibitor of PKC (by ~60%) than the longer version, but both were shown by biochemical assay to block selectively the complete range of isotypes present in PKC purified from whole brain (House and Kemp, 1987). The coding portion of the minigene was optimized for mouse codon usage. The entire L7-PKCI construct was linearized with HindIII and EcoRI and injected into fertilized mouse eggs using previously described methods (Oberdick et al., 1990).

Six positive transgenic mouse lines (FVB/N background) were identified by PCR analysis of DNA prepared from tail biopsies. Animals from all lines showed no gross behavioral deficits, displaying fluid and well-coordinated gross motor skills. By Northern blot analysis of total cerebellar RNA, two lines revealed no detectable expression of the transgene. The other four showed

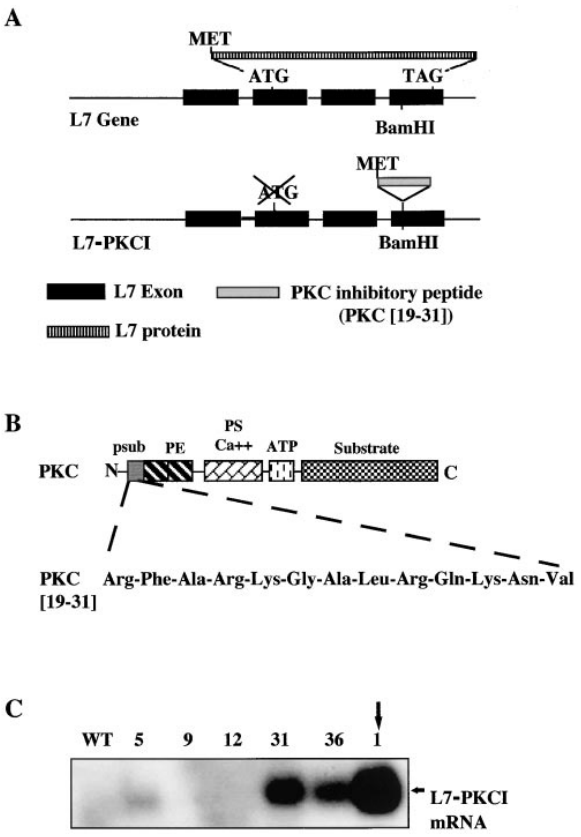

Figure 1. Construction and Expression of the L7-PKCI Transgene

(A) The normal *L7* gene is shown at the top. The L7-PKCI transgene construct (bottom) was made by insertion of a synthetic mini-gene coding for the peptide PKC[19–31] into the BamHI site of the vector L7ΔAUG (Smeyne et al., 1995). The latter vector is a version of the *L7* gene in which all potential start codons (ATG) in all reading frames were eliminated by PCR from all *L7* exons so that translation may only be initiated from a start codon (MET) provided within cDNAs inserted into the unique BamHI cloning site.

(B) Structure of the prototypical PKC and sequence of PKC[19–31]. This inhibitory peptide is part of the N-terminal pseudosubstrate domain (psub) of most PKC isotypes and negatively regulates PKC catalytic activity by mimicking substrate. Schematic was adapted from Newton, 1995. Abbreviations: PE, phorbol ester activation domain; PS, phospatidylserine and Ca^{2+} binding domain; and ATP, ATP binding domain.

(C) Northern blot analysis of RNA prepared from cerebella of wild-type and various L7-PKCI transgenic mouse lines. The blot was probed with a ^{32}P-labeled antisense oligonucleotide corresponding to the PKC[19–31] minigene. The line with highest expression (line 1, arrow) was used for all experiments described here, and the cell physiological data were confirmed in the next highest expressor (line 31).

variable levels of expression (Figure 1C). Although the precise time course of L7-PKCI transgene expression has not been determined here, it should be noted that endogenous L7 and its transgene derivatives such as L7-β-gal have been reported to be first detectable at embryonic day 15 and are continuously expressed into adulthood (Oberdick et al., 1993; Baader et al., 1998). Thus, it is expected that the L7-PKCI transgene would become activated not only after the final generation of Purkinje cells but also during their early differentiation and maturation.

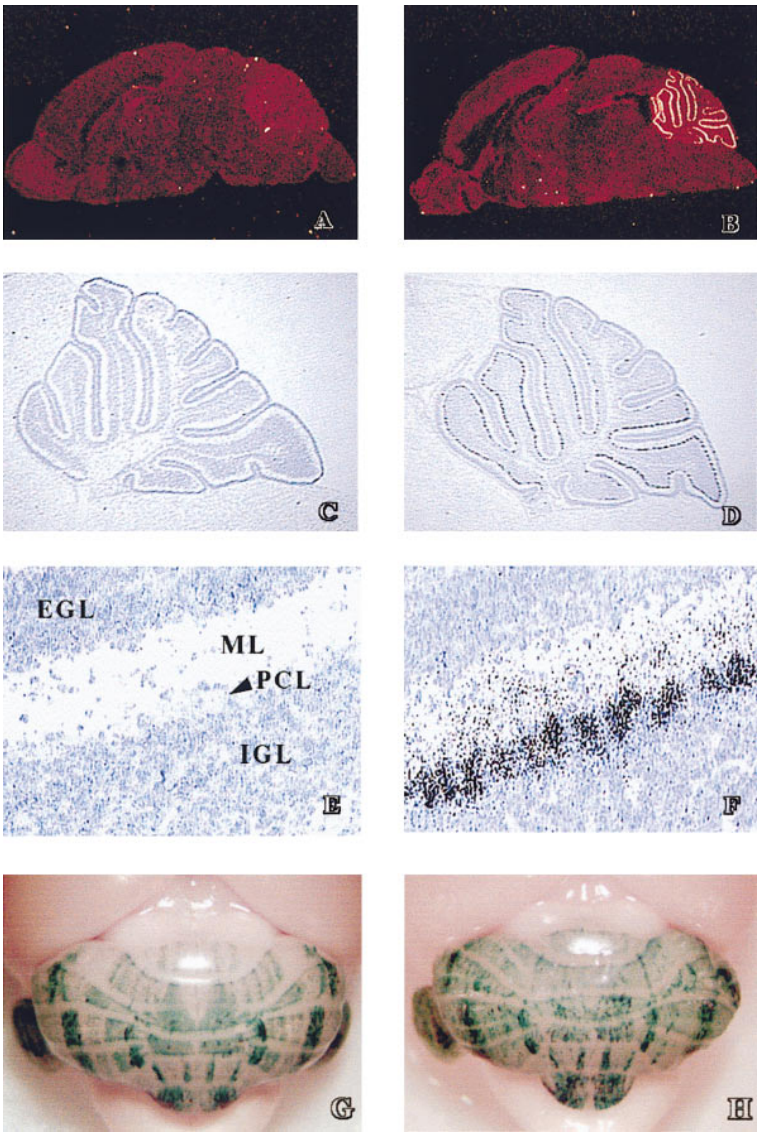

Figure 2. Purkinje Cell-Specific Expression of the L7-PKCI Transgene and Lack of Effect on Cerebellar Morphology

In situ hybridization was performed on sections of L7-PKCI and wild-type mouse brain using ^{35}S-labeled PKCI antisense oligonucleotide probe. Hybridization signal is undetectable in wild-type sections at all magnifications ([A], [C], and [E]) but is clearly detectable in the Purkinje cell layer of L7-PKCI sections ([B], [D], and [F]). (A) and (B) are dark-field views, whereas panels (C) through (F) are bright-field. Grains in the molecular layer in (F) are localized to Purkinje cell dendrites as reported previously for endogenous and transgene versions of the *L7* mRNA (Bian et al., 1996).

(G and H) Whole mount views of L7βG3 expression in wild-type (G) and L7-PKCI transgenics (H). The gross pattern of sagittal bands (blue-green β-gal stain) is unchanged. Likewise, the pattern of lobulation and fissurization is unchanged.

Magnifications: (A and B) 12.5×, (C and D) 30×, (E and F) 200×. Abbreviations: EGL, external germinal layer; ML, molecular layer; PCL, Purkinje cell layer; and IGL, internal granule cell layer.

The data reported below were collected using the highest expressor (line 1), or the second highest expressor (line 31), or both; the expression level of PKC[19–31] mRNA in line 31 is ~30% of that in line 1 (Figure 1C). Expression of the inhibitory peptide in Purkinje cells was confirmed by an electrophysiological assay of a phorbol ester-dependent effect that is attenuated in cerebellar cultures prepared from L7-PKCI mice (see below).

Anatomical Analysis of L7-PKCI Mice

By in situ hybridization, expression of the transgene mRNA was revealed to be specifically and abundantly localized to cerebellar Purkinje cells (Figure 2). No detectable expression was observed in any other brain region. All cerebellar laminae of L7-PKCI mice appeared to be of normal size and arrangement, and foliation was normal (Figures 2C, 2D, 2G, and 2H). Immunohistochemical staining with antibodies to the proteins calbindin (CaBP) (Jande et al., 1981) and L7 (Oberdick et al., 1988) revealed normal Purkinje cell morphology, number, and density in L7-PKCI mice as compared to wild types. The average area of cerebellar sections at the midline was 7.9 ± 0.4 mm^2 in wild-type versus 7.7 ± 0.4 mm^2 in L7-PKCI mice, whereas in the hemispheres it was 6.2 ± 0.5 mm^2 in wild-type versus 5.6 ± 0.3 mm^2 in L7-PKCI mice. The Purkinje cell density at the midline was measured to be 31 ± 6 PCs/mm in the wild-type and 34 ± 6 PCs/mm in L7-PKCI mice. Thus, none of these measures in L7-PKCI mice shows any significant difference from wild type.

The cerebellum is divided into a series of sagittally oriented modules, which can be revealed by tracing patterns of afferent and efferent projections as well as by electrophysiological properties of the Purkinje cell responses (Voogd and Bigaré, 1980; De Zeeuw et al., 1994). In L7-PKCI mice, a number of Purkinje cell markers that identify sagittal zones within the cerebellar cortex (L7-β-gal, Oberdick et al., 1993; zebrin II, Leclerc et al., 1992) were shown to have normal patterns of

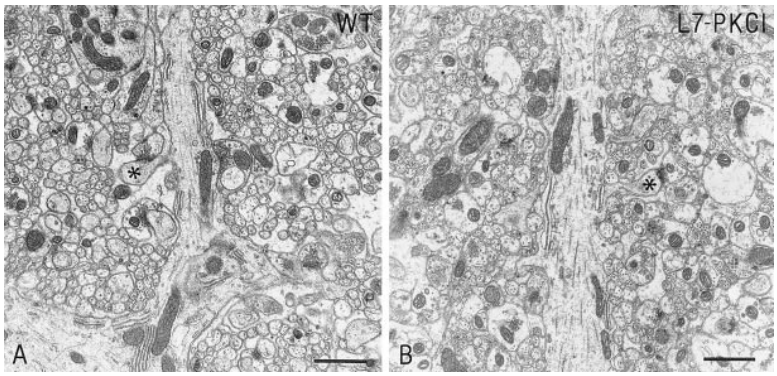

Figure 3. Ultrastructure of Parallel Fiber Synapses onto the Purkinje Cell Is Indistinguishable

The electron micrographs are from sagittal sections of the molecular layer in the vestibulocerebellum of wild types (A) and L7-PKCI mutants (B). Asterisks indicate the morphology of a Purkinje cell spine innervated by an asymmetric synapse. Scale bars, 1 μm.

expression. Similarly, sagittally organized granule cell patches that have been suggested to be dependent upon the pattern of mossy fiber innervation (nNOS, Schilling et al., 1994) were observed to be unaffected. These observations are summarized in Figures 2G and 2H, in which the pattern of expression of a truncated version of L7-β-gal is compared in wild-type and L7-PKCI backgrounds. Although subtle differences can be seen, these cannot be distinguished from effects due to individual and strain variability at this time. Nevertheless, it is quite clear that the gross pattern of sagittal banding is normal in L7-PKCI mice. Likewise, electron microscopic analysis of the neurons and interneurons in the cerebellar cortex in L7-PKCI mice showed no obvious abnormalities; although the total surface area comprised by glia may be somewhat larger in the mutant, the ultrastructural characteristics of the Purkinje cell dendritic trees and spines as well as their innervation by parallel fibers and GABAergic interneurons appeared both morphologically and numerically normal (Figure 3). In both wild types and L7-PKCI mutants, the majority of the terminals in the molecular layer of the cortex in the vestibulocerebellum contained clear round vesicles and established asymmetric synapses with Purkinje cell spines. The average density of these presumptive parallel fiber synapses was 22 ± 2.4 per 100 μm^2 and 19 ± 2.8 per 100 μm^2 in the wild types and L7-PKCI mutants, respectively. This difference was not significant. These findings suggest that the intrinsic patterning of Purkinje cells as well as the regulated patterning of mossy fiber to parallel fiber afferents are unaffected by L7-PKCI expression. However, it should be cautioned that while obvious alterations in the circuitry of the cerebellar cortex layer could not be seen, it is possible that there are subtle alterations of circuitry or subcellular structure that might elude the present morphological analysis (see Figure 8).

Electrophysiology of Purkinje Cells in Culture

When dispersed cultures were prepared from the cerebella of embryonic L7-PKCI and wild-type mice, no gross differences in cell morphology (size, number or ratio of cell types, degree or pattern of neurite outgrowth, degree of clustering) could be observed at the level of light microscopy (data not shown). Examination of a number of basal electrophysiological parameters revealed no significant differences between L7-PKCI and wild-type Purkinje cells. These included V_m (B6C3F1 wild type = −70 ± 4 mV, n = 6; L7-PKCI-[1] hetero/B6C3F1 = −73 ± 4 mV, n = 7; L7-PKCI-[31] hetero/FVB/N = −69 ± 5 mV, n = 5), R_{input}, (B6C3F1 wild type = 150 ± 26 MΩ, n = 6; L7-PKCI-[1] hetero/B6C3F1 = 159 ± 31 MΩ, n = 7; L7-PKCI-[31] hetero/FVB/N = 145 ± 38 MΩ, n = 5), mEPSC frequency (B6C3F1 wild type = 9.2 ± 3.0 s^{-1}, n = 8; L7-PKCI-[1] hetero/B6C3F1 = 8.5 ± 2.6 s^{-1}, n = 8; L7-PKCI-(31) hetero/FVB/N = 9.6 ± 3.6 s^{-1}, n = 6), and mEPSC amplitude (B6C3F1 wild type = 22 ± 6 pA, n = 8; L7-PKCI-[1] hetero/B6C3F1 = 21 ± 6 pA, n = 8; L7-PKCI-[31] hetero/FVB/N = 22 ± 7 pA, n = 6). mEPSC frequency and amplitude were measured over a 500 s recording period at a holding potential of −80 mV.

It is important to determine whether the PKCI peptide is expressed at levels sufficiently high to inhibit strongly PKC activity in Purkinje cells. A downside to the present anatomical specificity of transgene expression is that standard biochemical assays cannot always be employed even on carefully microdissected tissue. For example, even in microdissected cerebellar cortex, the Purkinje cells contribute only a minority of total PKC activity. Thus, strong inhibition of this PKC activity in Purkinje cells becomes difficult to detect in a background of PKC activity from other cell types. To circumvent this problem, we have utilized an electrophysiological assay. Activation of PKC by exogenous compounds such as phorbol esters and synthetic diacylglycerols has been shown to attenuate voltage-gated potassium currents in a number of cell types (Farley and Auerbach, 1986; Grega et al., 1987; Doerner et al., 1988), including rat cerebellar Purkinje cells grown in culture (Linden et al., 1992). We have replicated this observation using B6C3F1 wild-type mouse Purkinje cells (Figure 4) and have shown that the attenuation produced by phorbol ester (300 nM phorbol-12,13-diabutyrate; 41% ± 3.3% attenuation of peak current, n = 6 cells) is strongly blocked by a PKC inhibitor (chelerythrine, 10 μM; 7% ± 2.8% attenuation of peak current, n = 5 cells). The potassium current elicited in these recording conditions is likely to be predominantly composed of delayed outward rectifier current, although a contribution of A-current to the peak component is also possible. The attenuation seen herein takes the form of a decrease in conductance without an associated change in the voltage dependence of activation (data not shown). Most importantly, application of phorbol-12,13-dibutyrate to Purkinje cells derived from either L7-PKCI-(1) hetero/

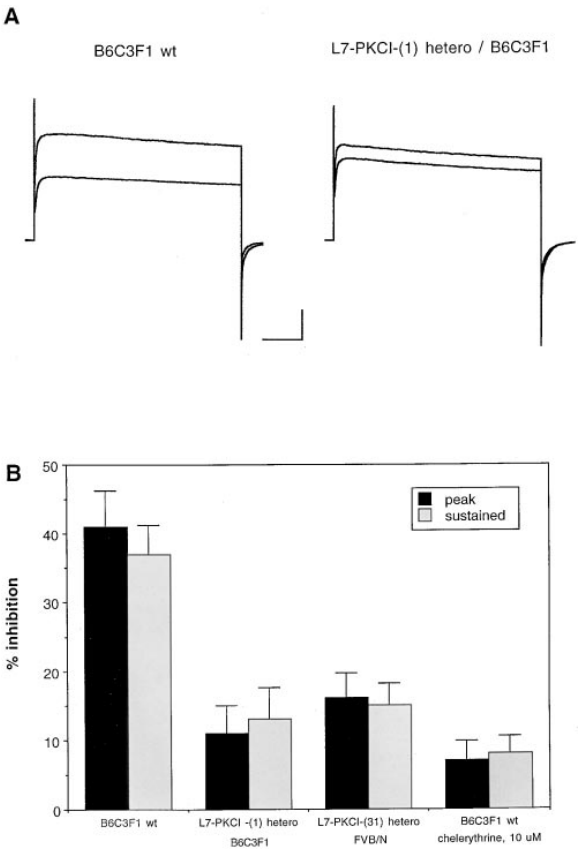

Figure 4. Attenuation of Potassium Currents by an Exogenous PKC Activator Is Blocked in L7-PKCI Purkinje Cells

(A) Families of outward currents were evoked by step depolarizations from a holding potential of −90 mV. The currents illustrated here were evoked with depolarizing steps to 40 mV and are single representative traces recorded immediately before (larger traces) and 10 min after the application of the PKC activator phorbol-12,13-dibutyrate (300 nM) in the bath (smaller traces). Scale bars, 1 nA, 50 ms.

(B) Summary graphs showing the degree of attenuation produced by phorbol-12,13-dibutyrate (300 nM) upon both the peak and sustained components of the outward current. B6C3F1 wild type, n = 6; L7-PKCI-(1) hetero/B6C3F1, n = 5; L7-PKCI-(31) hetero/FVB/N, n = 6; chelerythrine/B6C3F1 wild type, n = 5.

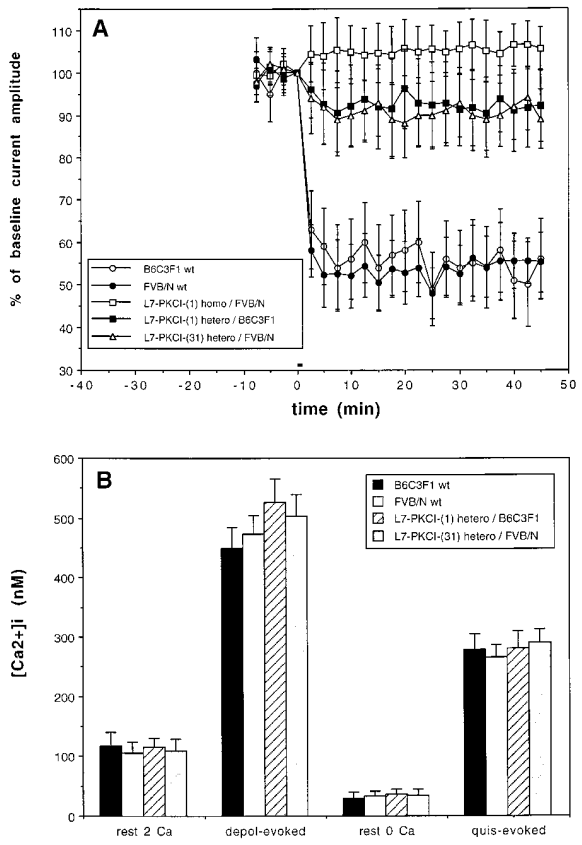

Figure 5. Induction of Cerebellar LTD Is Suppressed in Cultured Purkinje Cells Derived from L7-PKCI Mice

(A) Following acquisition of baseline responses to glutamate test pulses, glutamate/depolarization conjunction was applied at t = 0 min. LTD is induced in wild-type Purkinje cells of either the B6C3F1 (n = 7 cells) or the FVB/N mouse (n = 5). Purkinje cells derived from both homozygous L7-PKCI mice produced in a FVB/N background (n = 5) and heterozygous L7-PKCI mice produced in a B6C3F1 background (line 1; n = 6) or FVB/N background (line 31; n = 6) showed strong suppression of LTD.

(B) Control experiments to determine if PKCI expression produces its suppression of LTD induction through effects on Ca^{2+} influx and/or mobilization. Peak Ca^{2+} transients were measured in proximal dendritic shafts of Fura–2 loaded Purkinje cells grown in culture. Ca^{2+} transients evoked by a 3 s depolarization to 0 mV in normal (2 mM) external Ca^{2+} were measured as an index of voltage-gated Ca^{2+} channel function. Ca^{2+} transients evoked by a pulse of 100 μM quisqualate in 0 Ca^{2+}/0.2 mM EGTA external saline (6 psi, 2 s) were measured as an index of mGluR1 function. Heterozygous L7-PKCI mice produced in a B6C3F1 (line 1) or FVB/N (line 31) background were not significantly different from wild-type controls in either measure (n = 5 cells/group for depolarization-evoked Ca^{2+} influx and n = 10 cells/group for quisqualate-evoked Ca^{2+} mobilization).

B6C3F1 or L7-PKCI-(31) hetero/FVB/N mice produced only a minimal attenuation of the potassium current (11% ± 3.9% and 16% ± 3.6% attenuation of peak current, respectively; n = 5 cells/group), indicating that the expression of the PKCI peptide in these Purkinje cells is sufficient to strongly inhibit PKC.

If the induction of cerebellar LTD requires PKC activation, then this process should be blocked in L7-PKCI Purkinje cells. Cerebellar LTD was measured in voltage-clamped Purkinje cells in culture using a method in which parallel fiber stimulation was replaced by iontophoretic glutamate pulses and climbing fiber stimulation was replaced by direct depolarization of the Purkinje cell (Linden et al., 1991; reviewed by Linden, 1996). Following acquisition of baseline responses, glutamate/depolarization conjunctive stimulation was applied and glutamate test pulses were resumed to monitor the time course of Purkinje cell responses (Figure 5A). This treatment reliably induced LTD in Purkinje cells derived from two different strains of wild-type mice, B6C3F1, a pigmented strain, and FVB/N, an albino strain. In contrast, LTD was strongly attenuated in L7-PKCI Purkinje cells derived from either heterozygotes in the B6C3F1 (line 1) or FVB/N (line 31) background or homozygotes in the FVB/N (line 1) background. The effects were most prominent in the cells obtained from the homozygous

animals, but all Purkinje cells derived from the different transgenic cell lines or backgrounds revealed the same aberrations; all transgenic L7-PKCI mice showed a severe impairment of LTD induction.

To interpret more accurately the inhibitory effect of the L7-PKCI transgene on LTD induction, it became necessary to screen L7-PKCI Purkinje cells to determine if they had altered properties that might be expected to impact cerebellar LTD independent of a direct effect on PKC. As voltage-gated calcium channels (Sakurai, 1990; Linden et al., 1991; Konnerth et al., 1992) and mGluR1 receptors (Aiba et al., 1994; Conquet et al., 1994; Shigemoto et al., 1994) are known to be necessary for LTD induction, L7-PKCI Purkinje cells were screened to determine if they had alterations in either of these two signaling systems. Fura–2 microfluorimetry was used to assess depolarization-evoked Ca^{2+} influx in normal Ca^{2+} external saline (2 mM), as an index of voltage-gated Ca^{2+} channel function, and quisqualate-evoked Ca^{2+} mobilization in Ca^{2+}-free external saline as an index of mGluR function. Figure 5B illustrates that neither basal Ca^{2+}, nor increases evoked by Ca^{2+} influx via voltage-gated channels, nor Ca^{2+} mobilization via mGluR1 receptors is significantly altered in L7-PKCI heterozygotes in a B6C3F1 (line 1) or FVB/N (line 31) background.

Compensatory Eye Movements of L7-PKCI Mice

VOR Adaptation Is Affected

To determine whether L7-PKCI mice can show cerebellar motor learning, we investigated whether these mice adapt the gain of their VOR during visuo-vestibular training. Heterozygous L7-PKCI mice ($n = 8$) and wild-type littermates ($n = 10$) in the B6C3F1 (line 1) background were subjected to a training period of 1 hr of sinusoidal table stimulation (0.4 Hz; 3°/s peak velocity) and 180° out-of-phase drum stimulation (0.4 Hz; 3°/s peak velocity). The average gain of the eye movements of wild-type mice during VOR in the dark (VOR-D) at 0.4 Hz increased significantly ($p < 0.002$; Mann-Whitney rank sum test) from 0.21 ± 0.02 (mean ± SEM) before the training to 0.38 ± 0.04 after the training (thus, an average increase of 81%; for example, see Figure 6A). In contrast, the average gain of the eye movements of L7-PKCI mice during this protocol did not change significantly (from 0.25 ± 0.07 to 0.23 ± 0.03). The change in VOR gain after visuo-vestibular training as observed in the wild types was frequency specific (Figure 6B); the VOR gains at 0.1 Hz, 0.2 Hz, and 0.8 Hz were not significantly affected by the training. The adaptation only occurred at 0.4 Hz, the frequency at which the vestibular and visual training stimuli were provided. After the training protocol that was aimed at increasing the VOR gain, the same mice were subjected to a so-called suppression protocol in which the drum moved for 1 hr in phase with the table (both at 0.4 Hz; table and drum, 3°/s and 6°/s peak velocity, respectively). In wild-type mice this suppression protocol reduced the gain during VOR-D at 0.4 Hz significantly to 61% of the starting value ($p < 0.01$; Mann-Whitney rank sum test), whereas in L7-PKCI mice, no alterations of the VOR gain were observed (Figure 6C). This effect was also frequency specific. We conclude from these experiments that VOR adaptation in

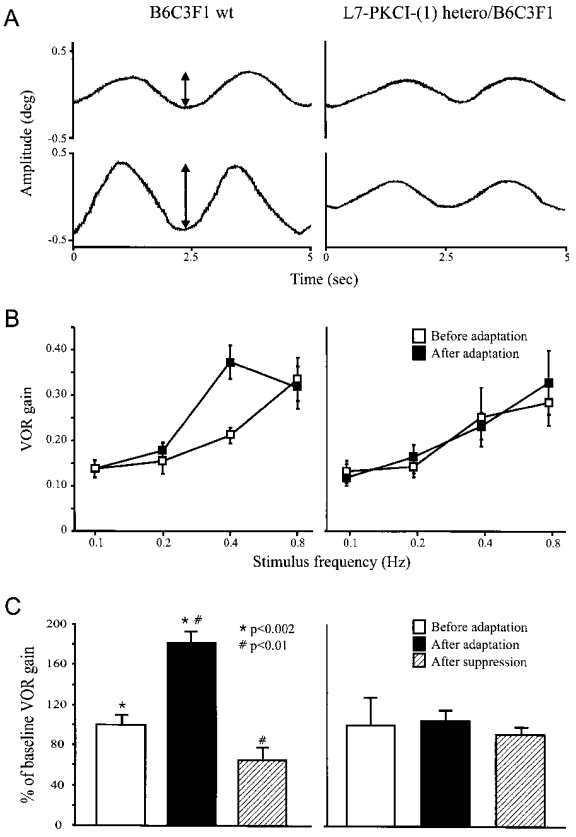

Figure 6. VOR Adaptation Is Impaired in L7-PKCI Mice

(A) The left panel illustrates the eye movements of a B6C3F1 wild-type mouse during turntable rotation at 0.4 Hz (peak velocity 3°/s) in the dark (VOR) before (top) and after (bottom) 1 hr of visuo-vestibular training. The right panel illustrates the eye movements of an L7-PKCI-(1) hetero/B6C3F1 littermate during the same protocols. Note that the gain of the wild-type animal increases after the training (compare arrow lengths), whereas the gain of the mutant remains the same.

(B) The adaptation of the gain is frequency specific. The increase of the VOR gain occurred only at 0.4 Hz, the frequency at which the training was performed.

(C) The VOR gain increase of the wild type at 0.4 Hz after adaptation could be converted into a decrease of the gain after subjecting the animal to a suppression protocol (1 hr of optokinetic stimulation in phase with turntable stimulation, left). In L7-PKCI mice, however, gain suppression was not possible (right). Thus, mice can increase or decrease their VOR gain following visuo-vestibular training in a frequency-specific manner, but this adaptation can occur only in the absence of the PKCI transgene. Note that in (A) the amplitude of the eye movement is given in degrees, in (B) the absolute gain values are presented, and in (C) the gain values are presented as percentages of the baseline gain (set at 100%) at the beginning of the adaptation or suppression training protocol.

B6C3F1 wild-type mice is frequency specific, that VOR adaptation can lead to both an increase and a decrease of the gain, and that both of these forms of VOR adaptation are attenuated by expression of the PKCI transgene in Purkinje cells.

General Eye Movement Performance Is Not Impaired

To determine whether the impaired VOR adaptation of the L7-PKCI mice is accompanied by general deficits in

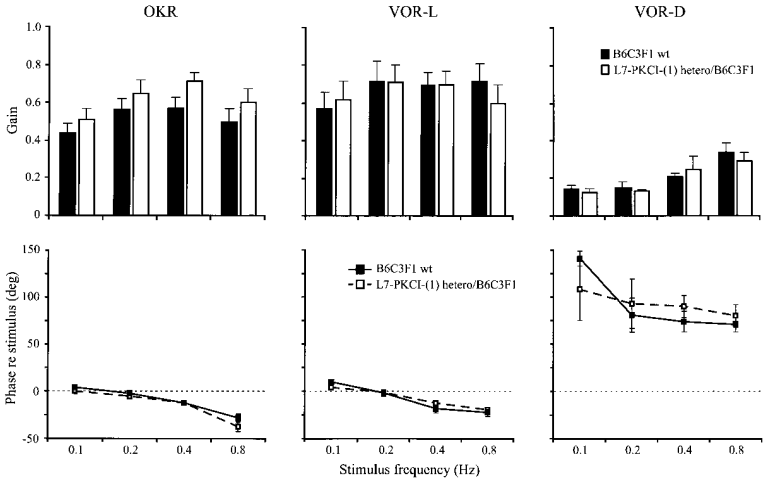

Figure 7. General Eye Movement Performance Is Not Impaired in L7-PKCI Mice

The gain (top) and phase (bottom) values of L7-PKCI-(1) hetero/B6C3F1 mice (n = 8) and B6C3F1 wild-type littermates (n = 10) were determined during OKR (left), VOR in the light (VOR-L; middle), and VOR in the dark (VOR-D; right) at four different stimulus frequencies. The gain and phase values of the L7-PKCI-(1) hetero/B6C3F1 mice did not differ significantly from those of the B6C3F1 wild types during any of the stimulus protocols. Thus, L7-PKCI mice are, as demonstrated in Figure 6, unable to adapt their VOR gain during an hour of visuo-vestibular training, but their initial gain values before the training are apparently indistinguishable from those of wild types. The phase values as presented in this figure did not change after the training sessions.

eye movement performance, we investigated the gain and phase during sinusoidal optokinetic and vestibular stimulation at different frequencies (0.1 Hz, 0.2 Hz, 0.4 Hz, and 0.8 Hz) and peak velocities (3°/s, 6°/s, and 9°/s). All gain and phase values of the eye movements of the L7-PKCI mice (B6C3F1 background, line 1; n = 8) during the optokinetic reflex (OKR), VOR in the light (VOR-L), and VOR-D were not significantly different from those of wild-type littermates (n = 10) over the range of frequencies and peak velocities examined (Figure 7). In the light (OKR and VOR-L), the gain of the eye movement of both mutants and wild types was generally above 0.5, the phase of the eye movement was lagging behind that of the stimulus, and the variations were small. In VOR-D, the gain of the eye movement of the animals was always below 0.5, the phase of the eye movement was leading that of the table, and the variations were relatively large as a consequence of the absence of visual stabilization. In addition, we investigated whether the latency of the optokinetic response to velocity step stimulation (0.1 Hz, 3°/s) was affected in mutants. The turnaround of the optokinetic response of the L7-PKCI mice followed on average 112 ± 8 ms (mean ± SEM) after the turnaround of the drum. This value was also not significantly different from the average latency of the eye movement response of the wild types (105 ± 10 ms). Thus, we conclude that the eye movement performance of L7-PKCI mice is not affected in that the amplitude (gain) and timing (phase and latency) of their compensatory eye movements are normal.

Climbing Fiber Innervation of Purkinje Cells in L7-PKCI Mice

It has previously been demonstrated that the global knockout of any one of a number of signaling molecules expressed in Purkinje cells results in an impairment of the developmental conversion from multiple to single innervation of Purkinje cells by climbing fibers (Kashiwabuchi et al., 1995; Kano et al., 1997). Of particular interest to the present study was the finding that this occurred in the global knockout of PKCγ (Chen et al., 1995; Kano et al., 1995). To determine whether sustained multiple climbing fiber innervation occurred in L7-PKCI mice, climbing fiber-evoked EPSCs were measured in whole-cell recordings from Purkinje cells in sagittal slices prepared from the vermis of L7-PKCI/B6C3F1 mice (line 1, age P21–P35) and age-matched B6C3F1 wild-type controls. Purkinje cells were voltage clamped at holding potentials positive to the resting potential and climbing fiber-mediated EPSCs were evoked by applying stimuli of varying intensities to the underlying white matter. Due to the all-or-none characteristics of climbing fiber responses, the number of discrete EPSC steps with varying stimulation strength can be used as an indicator for the number of climbing fibers innervating a Purkinje cell. The degree of multiple climbing fiber innervation of Purkinje cells in L7-PKCI transgenic mice was higher than in wild types (Figure 8). In slices prepared from both heterozygous (four of nine cells) and homozygous (three of six cells) L7-PKCI-(1)/B6C3F1 mice, approximately half of the Purkinje cells were innervated by two climbing fibers, whereas in B6C3F1 wild types only one in ten cells received a double innervation at this age. We did not observe multiple climbing fiber innervation of a higher order (triple, quadruple, etc.). The observation that there is a higher degree of multiple climbing fiber innervation of Purkinje cells in L7-PKCI transgenic mice suggests that PKC activity intrinsic to the Purkinje cell is involved in the synapse elimination process leading to the typical 1:1 innervation ratio in adult wild-type mice.

General Motor Performance of L7-PKCI Mice

The impaired elimination of the multiple climbing fiber innervation of Purkinje cells in the PKCγ knockout mice has been related to a concomitant impairment of motor performance as revealed by rotorod tests (Chen et al., 1995). Since the L7-PKCI mice also show sustained multiple climbing fiber innervation during adulthood, we subjected them to the same series of rotorod tests that were used previously to analyze the PKCγ knockout mice. The duration in which the animals remained on the apparatus (retention duration) was determined using L7-PKCI mice (B6C3F1 strain, line 1; n = 8) and wild-type littermates (n = 10) on the stationary rotorod, the running rotorod, and the stationary horizontal thin rod.

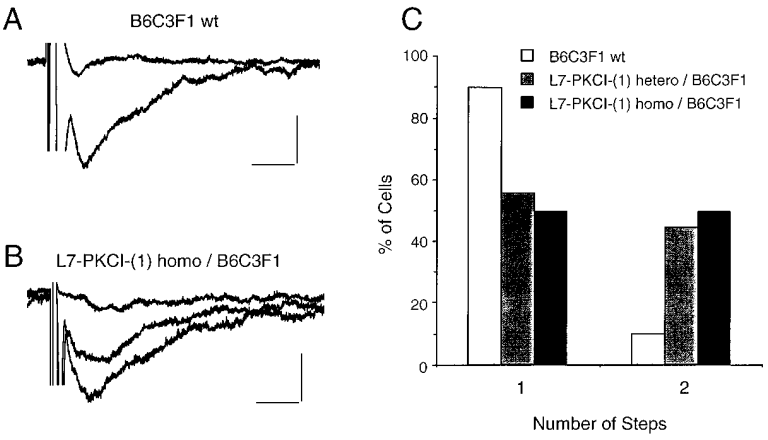

Figure 8. Impaired Elimination of Multiple Climbing Fiber Innervation of Purkinje Cells in L7-PKCI Mice

To measure climbing fiber-mediated EPSCs and to suppress complex spikes, the Purkinje cells were voltage clamped at holding potentials positive to the resting potential, typically between −30 mV and −40 mV.

(A) Example of a B6C3F1 wild-type Purkinje cell (P32) innervated by a single climbing fiber (holding potential, −40 mV).

(B) Example of an L7-PKCI homozygous Purkinje cell (P32) innervated by two climbing fibers (holding potential, −30 mV). In (A) and (B), averages of 3–8 responses are shown at each threshold intensity. Scale bars, 10 ms and 0.5 nA.

(C) Summary histogram indicating the proportion of single and double climbing fiber innervation in B6C3F1 wild-type (n = 10), L7-PKCI-(1) homo/B6C3F1 (n = 6), and L7-PKCI-(1) hetero/B6C3F1 (n = 9) mice. No higher order innervation (triple, quadruple, etc.) was seen.

Six trials were conducted. In none of these tests did the L7-PKCI mice differ significantly from the wild types (Figure 9). In all three tests the retention duration of both the L7-PKCI and the wild-type mice gradually increased over six trials from ~15 s to 50 s. As a positive control, we subjected adult *lurcher* mice (B6CBACa, n = 6), which lack Purkinje cells (Caddy and Biscoe, 1979), to the same rotorod tests. These mice completely lacked the ability to control their movements; in all three tests, their average retention duration remained between 0 and 10 s. We conclude from these experiments that sustained multiple climbing fiber innervation of the magnitude seen here does not necessarily result in impaired motor coordination.

Discussion

The main finding of this study is that specific expression of a PKC inhibitory peptide in the Purkinje cells of a transgenic mouse (L7-PKCI) resulted in nearly complete suppression of both cerebellar LTD as assessed in culture and adaptation of the VOR in the intact, behaving animal. The phenotype of these animals was remarkably delimited. Basal electrophysiological and morphological features of Purkinje cells were unaltered (with one notable exception discussed below). Likewise, these mice showed normal motor coordination as measured by their ability to display normal eye movement reflexes (OKR and VOR) as well as by several tests of gross motor coordination (rotorod, thin rod). Their behavioral deficit appeared to be limited to a particular form of motor learning: adaptation of the VOR. While there are a number of important limitations to the interpretation of this finding, we believe that it stands as the most compelling evidence to date in favor of the hypothesis that cerebellar LTD is necessary for this form of motor learning.

To control for the effects of genetic background and insertion site, electrophysiological measurements were made using mice constructed in two different genetic backgrounds, B6C3F1 hybrid and FVB/N inbred strains, using two independently derived transgenic lines, 1 and 31. In spite of the fact that line 31 expressed the L7-PKCI product at ~30% of the level of line 1, similar results were found in terms of our electrophysiological index of PKC inhibition (attenuation of the effect of phorbol ester on voltage-gated K^+ currents; Figure 4). These values were slightly, although not significantly, higher than those produced by a saturating concentration of an exogenous PKC inhibitor (chelerythrine, 10 μM). This suggests that the concentrations of PKCI produced in the Purkinje cells of both line 1 and line 31 mice are likely to be saturating. No significant differences were seen between L7-PKCI mice as a function of the line or genetic background. These include the amplitude of LTD and several basal properties of Purkinje cells, as well as depolarization- and mGluR-evoked Ca^{2+} transients. Interestingly, the suppression of LTD in cultured Purkinje cells from L7-PKCI-(1) homozygous/FVB/N mice was slightly more complete than that in cells from L7-PKCI-(1) heterozygous/FBN/N mice. It is unclear if this is related to expression levels of the PKCI peptide or to more complex side effects.

The most salient aspect of the present behavioral analysis is the specificity of the phenotype in the L7-PKCI mice; VOR adaptation was robustly affected, whereas the general eye movements and general motor performance were not impaired. When the visuo-vestibular training was done at a relatively high frequency, as in the present study (cf. Koekkoek et al., 1997), the VOR adaptation in wild-type mice was frequency specific. This frequency-specific adaptive effect has also been described for higher mammals such as cats and primates (Lisberger et al., 1983; Powell et al., 1991). This specificity of VOR adaptation might be related to the fact that LTD is restricted to those parallel fiber-Purkinje cell synapses that were activated during LTD induction (Ekerot and Kano, 1985; Linden, 1994; but see Hartell, 1996). Certain mossy fibers and parallel fibers may very well be clustered in groups that carry particular head velocity signals, so that LTD will only occur at the Purkinje cell dendritic sites that are innervated by those

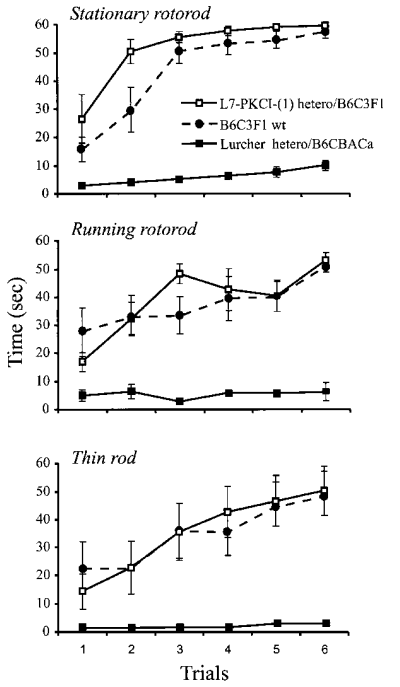

Figure 9. L7-PKCI Mice Show No General Motor Coordination Deficits

L7-PKCI-(1) hetero/B6C3F1 mice (n = 8) and B6C3F1 wild-type littermates (n = 10) were put on the stationary rotorod (top), the running rotorod (middle), and the stationary horizontal thin rod (bottom) for a maximum of 60 s for each trial. In all tests, the duration of retention on the apparatus gradually increased over the six trials for both groups. In none of the tests did the duration of retention of the L7-PKCI mice differ significantly from the wild types. For comparison, the staying duration times of *lurcher* mice, which show severe impairment of motor coordination, have been added.

parallel fibers activated under the stimulus frequency used for the training. This is consistent with the "flocculus hypothesis" of Ito and coworkers (1982).

While the main finding of this study is that specific blockade of cerebellar LTD correlates with specific blockade of VOR adaptation, it is also useful to consider the range of motor behaviors that remain intact when cerebellar LTD is blocked. The fact that the initial gain values of the L7-PKCI mice during all protocols, i.e., OKR, VOR-L, and VOR-D, were normal indicates that cerebellar LTD is not necessary for normal eye movement performance. Apparently, there is sufficient plasticity in the brainstem of the L7-PKCI mouse to obtain normal gain values when prolonged periods of training are available (Khater et al., 1993; Lisberger, 1994). Therefore, we hypothesize that it is only when the VOR adaptation has to occur rapidly (in our protocol, 1 hr), that PKC activity and LTD are necessary. Similarly, the general motor performance as revealed by initial performance in the rotorod and thin rod tests is not affected even though LTD is abolished. Thus, in contrast to previous reports (e.g., Aiba et al., 1994), it is unlikely that a lack of LTD can explain cerebellar ataxia. Furthermore, L7-PKCI animals improve with repeated trials of these tasks in a manner that is indistinguishable from wild-type controls. Thus, these forms of motor learning are unlikely to require cerebellar LTD. It will be useful to expand the behavioral analysis to other motor learning tasks, particularly associative eyeblink conditioning.

The role of LTD in cerebellar motor learning, as proposed in the Marr-Albus-Ito theories, has remained controversial (Lisberger, 1988; De Schutter, 1995, 1997; Simpson et al., 1996; Llinás et al., 1997). This debate is partly due to the fact that lesion studies have often been difficult to interpret. For example, lesions of the flocculus of the vestibulocerebellum, which is the region controlling compensatory eye movements, do not only affect VOR adaptation, but also general eye movement performance characteristics such as its phase dynamics or latencies (Robinson, 1976; Zee et al., 1981; Ito et al., 1982; Nagao, 1983; Koekkoek et al., 1997). Similarly, although homologous recombination knockout technology has made it possible to test the role of various signaling molecules in cerebellar LTD, it has been difficult to rule out contributions from noncerebellar systems or from multiple neuronal types within the cerebellum to behavioral phenotypes. For example, while mice null for the genes encoding mGluR1 (Aiba et al., 1994; Conquet et al., 1994), GluRδ2 (Funabiki et al., 1995; Kashiwabuchi et al., 1995), and glial fibrillary acidic protein (Shibuki et al., 1996) all showed impaired cerebellar LTD and some form of motor learning, the first two showed motor coordination deficits when the last did not. In none of these mutants was the cerebellar cortex the only brain location modified. Thus, mechanical and genetic lesion studies often result in conflicting behavioral deficits that may be explained by the complexity of cellular targets.

Another problem that has hindered investigations on the role of LTD in cerebellar motor learning is isotypic compensation. In this respect, the PKCγ knockout mouse is probably the most relevant. Despite the abundance of PKCγ in Purkinje cells, neither LTD induction nor associative eyeblink conditioning are impaired in these knockout mice (Kano et al., 1995). This fact may be due to compensation by one or more of the five other PKC isoforms (PKCα, βI, δ, ϵ and ζ) that have been reported by various laboratories to occur in Purkinje cells (Young, 1988; Shimohama et al., 1990; Wetsel et al., 1992; Chen and Hillman, 1993; Merchenthaler et al., 1993; Garcia and Harlan, 1997).

While these two major difficulties may have been alleviated in L7-PKCI mice, there are several caveats that should be sounded about the interpretation of the present results. First, while expression of the L7-PKCI transcript could be detected using in situ hybridization only in cerebellar Purkinje cells, it is possible that it is expressed at very low levels in other regions as well. For example, the endogenous *L7* gene is also expressed in retinal bipolar neurons (Oberdick et al., 1990). However, because L7-driven transgene expression in the retina is only rarely observed using the L7ΔAUG vector (unpublished data), L7-PKCI expression in the retina of both lines reported here is undetectable, and the optokinetic responses of transgenics were totally normal, this possibility is remote. Second, it cannot be absolutely determined whether the blockade of LTD in the L7-PKCI mouse results directly from inhibition of PKC. Whereas strong expression of the PKCI transcript is found in Purkinje cells, and whereas voltage-gated K^+ currents

in L7-PKCI Purkinje cells show the same response to a PKC activator as do wild-type Purkinje cells treated with an exogenously applied PKC inhibitor, the PKCI effect could be mediated by a secondary pathway not considered in this report (e.g., the NO/cGMP cascade; reviewed by Linden, 1996; Lev-Ram et al., 1997). Third, the one basal physiological abnormality that we have found in L7-PKCI mice is that ~50% of the Purkinje cells show a persistent multiple climbing fiber innervation, raising the possibility that this could be a cause of their failure to demonstrate VOR adaptation. We believe this to be unlikely because the PKCγ knockout mouse shows multiple climbing fiber innervation with normal cerebellar LTD and no motor learning deficit (Chen et al., 1995; Kano et al., 1995). Finally, while our search for basal abnormalities in the physiology and anatomy of the cerebellar cortex has been extensive, many of the experiments have been performed in a culture system, which limits the type of information obtained. It will be instructive to measure some physiological parameters of Purkinje cells (e.g., simple and complex spike firing rates) in situ, particularly in the behaving animal.

Persistent innervation of Purkinje cells by multiple climbing fibers is a phenotype that is found in a fairly large number of naturally occurring and induced mutant mice. In the PKCγ knockout mouse, this abnormality results from a diminished regression of multiple climbing fiber innervation in the third postnatal week (Kano et al., 1995), which is when PKCγ expression in Purkinje cells reaches its highest level (Yoshida et al., 1988; Huang et al., 1990). It was also noted that the number of parallel fibers innervating Purkinje cells in PKCγ mutant mice is normal. This is different from spontaneous mutants such as the *weaver* (Crepel and Mariani, 1979), *reeler* (Mariani et al., 1977), and *staggerer* (Crepel et al., 1980), as well as the GluRδ2 knockout mouse (Kashiwabuchi et al., 1995), in which the number of parallel fibers is substantially reduced. These observations led Kano et al. (1995) to propose that PKCγ may act as a downstream element in the signal cascade inside Purkinje cells necessary for the elimination of surplus climbing fiber synapses. The present observation, that chronic inhibition of PKC in Purkinje cells leads to persistent multiple climbing fiber innervation of Purkinje cells without affecting the morphology of parallel fiber input, is consistent with this hypothesis.

The level of multiple climbing fiber innervation in adult L7-PKCI mice is comparable to that of adult PKCγ mutants. In adult L7-PKCI mice, 47% of the Purkinje cells are innervated by two climbing fibers, whereas in the PKCγ knockout, 41% of the Purkinje cells are innervated by two or three (<5%) climbing fibers (Kano et al., 1995). The persistent multiple climbing fiber innervation in PKCγ mutant mice has been suggested to underlie their impaired motor coordination (Chen et al., 1995). This association is supported by reports of impaired motor coordination in mGluR1 (Aiba et al., 1994; Conquet et al., 1994) and GluRδ2 (Kashiwabuchi et al., 1995) mutant mice, in which, respectively, 25% and 46% of the Purkinje cells receive a multiple climbing fiber innervation. Conversely, glial fibrillary acidic protein knockout mice, which have impaired cerebellar LTD, show normal mono climbing fiber innervation and motor coordination (Shibuki et al., 1996). However, the present study demonstrates that a persistent multiple climbing fiber innervation does not necessarily result in impaired motor coordination. The adult L7-PKCI mutant mice do not show any sign of ataxia, and they display normal motor coordination skills in two different sets of tests, the eye movement tests and the rotorod/thin rod tests. One of the reasons for this discrepancy may be related to the fact that the other induced mutants are global knockouts, in which brain locations other than the cerebellar Purkinje cells are affected. For example, PKCγ is also expressed in the hippocampus, amygdala, and cerebral cortex (Huang et al., 1989), GluRδ2 is also expressed in the cingulate cortex and hippocampus (Lomeli et al., 1993), and mGluR1 is also expressed in the olfactory bulb, hippocampus, lateral septum, thalamus, globus pallidus, preoptic nucleus, substantia nigra, dorsal cochlear nucleus, striatum, islands of Calleja, cerebral cortex, mammillary nuclei, red nucleus, and superior colliculus (Shigemoto et al., 1992). Thus, it is likely that the defects in motor coordination seen in these global knockouts are not solely a result of multiple climbing fiber innervation and may reflect dysfunction in other brain regions. Another explanation for the robust motor coordination deficits in mice deficient in mGluR1 or GluRδ2 could be that their Purkinje cells have additional intrinsic deficits apart from the multiple climbing fiber innervation. However, it should be cautioned that rotorod/thin rod tests do not comprise a complete assay of motor coordination. While peformance of GluRδ2 and PKCγ knockouts versus L7-PKCI mice on these tests are dramatically different, it remains formally possible that there is a more sensitive test that would reveal motor coordination impairments in all three types of animal.

The present strategy has produced a transgenic mouse that bypasses two of the problems inherent in conventional gene knockouts: anatomical specificity and functional compensation from other members of the gene family. Another way to overcome the problem of anatomical specificity has been to use the phage P1-derived Cre/loxP recombination system, which allows the creation of a subregion and cell type-restricted gene knockout. This has been demonstrated in a study which examined the role of NMDAR1 receptors of hippocampal CA1 pyramidal cells in the formation of spatial memory (Tsien et al., 1990b, 1996a; Stevens, 1996). However, generating such mutants demands laborious screening of numerous cell lines, and this approach does not reduce the possibility that compensatory mechanisms of other related genes come into play. Both the present strategy and the Cre/loxP strategy will benefit greatly from coupling to inducible promoters (Mayford et al., 1996), which should attenuate the remaining problem of developmental side effects.

Experimental Procedures

Production of L7-PKCI Mice

The L7-PKCI vector was constructed by insertion of a 54 bp synthetic double-stranded DNA fragment into the BamHI site of pL7ΔAUG (Smeyne et al., 1995). No protein epitope tag was included

in this construct because of unpredictable effects on peptide function. The sequences of the two complementary 50 bp oligonucleotides are as follows: PKCI sense, 5′-GATCATGAGGTTCGCCAG GAAGGGCGCCCTGAGGCAGAAGAACGTGTAAG-3′; PKCI anti, 3′-TACTC CAAGCG GTCCTTCCCGCG G GACTCCGTCTTCT TGCACAT TCCTAG-5′.

The resulting plasmid was digested with HindIII and EcoRI, and the linearized construct was separated from the pGEM3 base plasmid by electrophoresis followed by electroelution. This purified fragment was used for injection into mouse embryos. The antisense oligo used to make the PKCI fragment was used as a probe in the Northern blot and in situ hybridization analyses. Northern blots were prepared as previously described (Bian et al., 1996).

Mouse Strains

The L7-PKCI founder mice were generated in the FVB/N strain (Taconic). Initial physiology and LTD tests were performed on homozygotes and heterozygotes in this strain background. As this strain is albino, F2 heterozygotes were crossed into a pigmented hybrid strain (B6C3F1 hybrids; Jackson Laboratory) for behavioral studies. The results reported here represent data collected from first generation pigmented animals as well as second and third generations; each successive generation was produced from a cross between a transgenic heterozygote and a stock wild-type B6C3F1 hybrid (thus yielding wild-type and transgenic littermates). Positive transgenic mice were identified by PCR using DNA prepared from tail biopsies. To confirm the cell physiological data were in the same strain as was used for the behavioral studies, second generation pigmented heterozygotes were mated to produce homozygotes in a complex B6C3F1 substrain. These were subsequently mated to B6C3F1 wild-type stock animals to produce heterozygous embryos for primary dissociated cultures and cell electrophysiological studies. All anatomical characterizations were performed in the B6C3F1 hybrid background.

Anatomical Analysis of L7-PKCI Mice

In Situ Hybridization

The in situ hybridization procedure was as reported previously (Smeyne et al., 1995; Bian et al., 1996). Antisense PKCI probe was end "tailed" with [^{35}S]dATP using terminal deoxynucleotidyl transferase. After development of photographic emulsion-dipped slides, sections were counterstained with cresyl violet. Images in Figure 2 were captured off of a Zeiss Axiophot microscope using an Optronix video camera and IPLab Spectrum software (Signal Analytics, Virginia).

Immunocytochemistry and L7-β-gal Analysis

Sections were reacted and processed with antibodies to L7, calbindin, and zebrin II (courtesy of Dr. Richard Hawkes) using methods reported previously (Baader et al., 1998). Sections were processed histochemically for NADPH-diaphorase as before (Schilling et al., 1994). L7-PKCI mice of line 1 were crossed to L7BG3 mice for analysis of L7-β-gal banding patterns. The latter transgenic mouse carries an L7-*lacZ* fusion transgene with a truncated (0.5 kb) promoter as previously described (Oberdick et al., 1993). Tissues were processed for *lacZ* in whole mount as reported previously (Oberdick et al., 1993).

Cell Counts and Area Measurements

For area measurements and Purkinje cell counts, 18 μM sagittal frozen sections were prepared on a cryostat (every fourth section was collected) and stained with cresyl violet. Four sections at the midline and four sections in the hemispheres (at the point just lateral to where lobule X disappears) were analyzed. Area measurements were made using IPLab Spectrum software (Signal Analytics, Virginia). The area measurements were confirmed in a second pair of animals. Purkinje cell density measurements were made by using IPLab software to define a linear segment in the Purkinje cell layer in the region to be counted. Three sections were counted from the cerebellar midline of both a wild-type and an L7-PKCI mouse, and three regions were counted in each section: the anterior lobe fissure between lobules III and IV/V, the central lobe fissure between lobules VII and VIII, and the fissure between lobules IX and X. The numbers in the text are averages of all sections and regions (nine counting events per genotype).

Electron Microscopy

The cerebella of three L7-PKCI mice (B6C3F1, line 1) and three wild-type littermates were processed for electron microscopy as described (De Zeeuw et al., 1997). In short, the mice were anesthetized with Nembutal (60 mg/kg) and perfused transcardially with 10 ml 0.9% saline in 0.1 M cacodylate buffer (pH 7.3), followed by 25 ml of 3% glutaraldehyde and 1% paraformaldehyde in the same buffer. The cerebella were sectioned in three different directions (i.e., sagittally, coronally, and transversely) on a Vibratome at 70 μm, osmicated, block stained in uranyl acetate, directly dehydrated in dimethoxypropane, and embedded in Araldite. Guided by observations made in the semi-thin sections, pyramids of different cerebellar lobules were prepared. From these tissue blocks, ultrathin sections were cut and mounted on Formvar coated nickel grids; most of these grids were processed for standard electron microscopy, but some were processed for GABA-immunocytochemistry (for details, see De Zeeuw et al., 1989). The latter grids were rinsed in a solution of 0.5 M Tris buffer containing 0.9% NaCl and 0.1% Triton X-100 (pH 7.6) (TBST) and incubated overnight at 4°C in a droplet of GABA antiserum (1:1000 in TBST). The GABA antiserum was generously supplied by Dr. R.M. Buijs (Buijs et al., 1987). The next day, the grids were rinsed twice with TBST (pH 8.2) and incubated for 1 hr at room temperature in a droplet of goat anti-rabbit IgG labeled with 15 nm gold particles (Aurion) diluted 1:25 in TBST. All grids were washed twice with TBST (pH 7.6) and distilled water, counterstained with uranyl acetate and lead citrate, and examined in a Philips electron microscope (CM-100). Random samples of parallel fiber terminals and GABAergic interneuron terminals were collected from at least three nonserial ultrathin sections obtained from at least two embedded tissue blocks of the vestibulocerebellum of each animal.

L7-PKCI Purkinje Cells in Culture

Embryonic mouse cerebellar cultures were prepared and maintained according to the method of Schilling et al. (1991). Cultures were maintained in vitro for 8–16 days at the time of use in electrophysiological experiments. Patch electrodes were attached to Purkinje cell somata and were used to apply a holding potential of −80 mV. Iontophoresis electrodes (1 μm tip diameter) were filled with 10 mM glutamate in 10 mM HEPES (adjusted to pH 7.1 with NaOH) and were positioned ~20 μm away from large-caliber dendrites. Test pulses were delivered using negative current pulses (600–800 nA, 30–110 ms duration) applied at a frequency of 0.05 Hz. After acquisition of baseline responses, six conjunctive stimuli were applied at 0.05 Hz, each consisting of a glutamate test pulse combined with a 3 s long depolarization step to 0 mV, timed so the depolarization onset preceded the glutamate pulse by 500 ms. Cells were bathed in a solution that contained (in mM): 140 NaCl, 5 KCl, 2 $CaCl_2$, 0.8 $MgCl_2$, 10 HEPES, 10 glucose, 0.005 tetrodotoxin, and 0.1 picrotoxin. The solution was adjusted to pH 7.35 with NaOH, which flowed at a rate of 0.5 ml/min. The recording electrode contained (in mM): 135 CsCl, 10 HEPES, 1 EGTA, and 4 Na_2-ATP, adjusted to pH 7.35 with CsOH. Patch electrodes yielded a resistance of 3–5 MΩ when measured with the internal and external salines described above. Membrane currents were recorded with an Axopatch 200A amplifier in resistive voltage-clamp mode, low-pass filtered at 5 kHz, and stored on a chart recorder. For potassium current recordings (Figure 4), $CaCl_2$ was removed from the external saline, and the internal saline contained (in mM): 140 KCl, 11 EGTA, 1$CaCl_2$, 10 HEPES, and 2 Na_2-ATP, adjusted to pH 7.35 with KOH. These currents were low-pass filtered at 2 kHz and digitized at 5 kHz using Axodata software (Axon Instruments). Fura–2 ratio imaging of intracellular free Ca^{2+} was accomplished by measuring the background corrected fluorescence ratio at 340 and 380 nm excitation using a cooled CCD camera system as previously described (Linden et al., 1995). Exposure times were 100–400 ms per single wavelength image. Experiments were conducted at room temperature.

Eye Movement Recordings

Eye movements were recorded with the use of the search coil method for mice (Koekkoek et al., 1997; De Zeeuw et al., 1998). General anesthesia was induced and maintained with a mixture of Ketamine (50 mg/ml) and Xylazine (2.8 mg/ml) in sodium chloride

(3.6 mg/ml). The initial dose was 0.07 ml i.p. supplemented with 0.03 ml i.p. every 35 min. After an incision was made in the skin, four holes with a diameter of 0.8 mm were drilled in the parietal and frontal bones, and stainless steel screws (M1, 3.75 mm long) were dipped in cyanoacrylate and screwed into the holes. A pedestal made of dental cement (Simplex Rapid, Austenal Dental Products LTD, England) containing two M3 fixation bolts and a two-pin connector was mounted on top of the screws with dental cement so that the flat top surface of the pedestal was placed at an angle of 15° with the nasal bone. The next day the animals were reanesthetized with Halothane (1 part O_2, 2 parts N_2O, and 2% Fluothane at a flow of 1.5 l/min; Zeneca, Ridderkerk), local eye anesthesia (Novesine, 0.4%; Bournonville-Pharma B.V., the Netherlands) was applied, and a pre-wound eye coil (2.8 mm outside diameter; Sokymat SA, Switzerland) made of 80 windings of 25 μm isolated brass wire (resistance of 25–35 Ω) was placed flat on the eye and carefully positioned in such a way that the pupil was located exactly in the center of the coil. The coil was fixed on the sclera with three 10–0 Ethilon monofilament sutures, and the wrapped coil wires were led underneath the skin toward the connector. Directly after surgery, the mouse was put in a restrainer with its pedestal surface fixed at 45° to the earth's horizontal (i.e., the angle between the nasal bone and the earth's horizontal was 60°) inside an electromagnetic measurement system (Skalar Medical). While the head-fixed animal was still anesthetized, the eye coil was calibrated in two different manners: by rotating the animal inside the fixed coil system as well as by rotating the coil system around the animal fixed in space. Subsequently, the animal was allowed to recover, and the recordings were started as soon as the animal was fully alert. The optokinetic and vestibular stimuli were given with the use of a servo-controlled turntable and a drum with different black and white stripes with a width corresponding to a visual angle to the mouse of 4°. The diameter and height of the drum were 24 cm and 20 cm, respectively. When the eye of the mouse was positioned in the center of the drum, the visual field provided by the drum extended from 33° below to 90° above the horizontal plane through the eye of the mouse. The stimulus frequency and amplitude were controlled by a personal computer with the use of the Spike2 for Windows Sequencer program and a CED machine (G. Smith; Cambridge Electronics Design). Eye, table, and drum position were monitored on storage oscilloscopes and recorded on-line using the CED 1401 signal capture device and Spike2 for Windows. The stimulus protocols included optokinetic stimulation and table stimulation in the dark and light, both before and after visuo-vestibular training. We used alternating constant velocity stimulation to measure latency, and sinusoidal stimulation to measure gain and phase of the eye movements. All tests were performed at frequencies and with peak velocities ranging from 0.1 Hz to 0.8 Hz and 3°/s to 9°/s, respectively. Each protocol contained at least 12 cycles enabling us to average gain, latency and phase values over at least 3 cycles without saccadic eye movements. Adaptation was induced by rotating the drum at 0.4 Hz either in counterphase (gain increase) or in phase (gain suppression) with the turntable at twice the amplitude (6°/s) for 1 hr. The effects of the adaptation were measured during VOR in the dark. All values were analyzed offline using the Ced-Anal program for Windows according to standard procedures (De Zeeuw et al., 1995).

Slice Preparations from L7-PKCI Cerebella

Sagittal slices of the cerebellar vermis (200–250 μm thick) were prepared from P21-P35 mice of the B6C3F1 strain. Following a recovery period, they were placed in a submerged chamber perfused with a bath solution containing (in mM): 124 NaCl, 5 KCl, 1.25 Na_2HPO_4, 2 $MgSO_4$, 2 $CaCl_2$, 26 $NaHCO_3$ and 10 D-glucose bubbled with 95% O_2 /5% CO_2 at room temperature. Recording was performed using the visualized whole-cell patch-clamp technique. Recording pipettes (resistance, 2–3 MΩ) were filled with a solution containing (in mM): 9 KCl, 10 KOH, 120 K gluconate, 3.48 $MgCl_2$, 10 HEPES, 4 NaCl, 4 Na_2-ATP, 0.4 Na_3-GTP, and 17.5 sucrose. Membrane currents were recorded with an Axoclamp-2A amplifier in continuous SEVC mode. Climbing fibers were stimulated in the white matter/granule cell layer using a monopolar tungsten electrode.

Motor Coordination Tests

The rotorod tests were performed according to the protocol described by Chen et al. (1995). The rotorod consists of a smooth plastic roller (8 cm diameter, 14 cm long) flanked by two large round plates (30 cm diameter) to prevent animals from escaping. A mouse was placed on the roller, and the time it remained on the stationary or rotating roller was measured. A maximum of 60 s was allowed for each animal for all motor skill tests. The thin rod consists of a smooth plastic rod (1.5 cm diameter, 50 cm long) held horizontally on both ends. A mouse was placed in the midpoint of the rod, and the time it remained on the rod was measured.

Acknowledgments

The authors would like to thank M. M. Morpurgo, J. v.d. Burg, R. Hawkins, E. Goedknegt, E. Dalm, D. Gurfel and E. Bugharin for technical assistance; J. Parker-Thornburg for construction of the L7-PKCI transgenic mouse lines; S. Baader for statistical analysis of cerebellar morphology; W. Russo and L. Eastman for animal care; and C. Aizenman and K. Takahashi for useful discussion. This research was supported by the Life Sciences Foundation (SLW; number 805–33.310-p; C.I.D.Z.), which is subsidized by the Netherlands Organization for Scientific Research (NWO); by a NWO project grant (number 903–68–361; C.I.D.Z.); by PHS MH51106, the Develbiss Fund, the McKnight Foundation, and the National Alliance for Research on Schizophrenia and Depression (D. J. L.); by the Deutsche Forschungsgemeinschaft (C. H.); and by NIH 1RO1NS33114 and NSF IBN-9309611 (J. O.).

Received December 11, 1997; revised January 13, 1998.

References

Aiba, A., Kano, M., Chen, C., Stanton, M.E., Fox, G.D., Herrup, K., Zwingman, T.A., and Tonegawa, S. (1994). Deficient cerebellar long-term depression and impaired motor learning in mGluR1 mutant mice. Cell *79*, 377–388.

Baader, S.L., Sanlioglu, S., Berrebi, A.S., Parker-Thornburg, J., and Oberdick, J. (1998). Ectopic overexpression of Engrailed-2 in cerebellar Purkinje cells causes restricted cell loss and retarded external germinal layer development at lobule junctions. J. Neurosci. *18*, 1763–1773.

Bian, F., Chu, T., Schilling, K., and Oberdick, J. (1996). Differential mRNA transport and the regulation of protein synthesis: selective sensitivity of Purkinje cell dendritic mRNAs to translational inhibition. Mol. Cell. Neurosci. *7*, 116–133.

Blendy, J.A., Kaestner, K.H., Schmid, W., and Schutz, G. (1996). Targeting of the CREB gene leads to up-regulation of a novel CREB mRNA isoform. EMBO J. *15*, 1098–1106.

Buijs, R.M., Van Vulpen, E.H.S., and Geffard, M., (1987). Ultrastructural localization of GABA in the supraoptic nucleus and the neural lobe. Neuroscience *20*, 347–355.

Caddy, K.W.T., and Biscoe, T.J. (1979). Structural and quantitative studies on the normal C3H and lurcher mutant mouse. Phil. Trans. R. Soc. (Lond.) *287*, 167–201.

Chen, S., and Hillman, D. (1993). Compartmentation of the cerebellar cortex by protein kinase C delta. Neuroscience *56*, 177–188.

Chen, C., and Tonegawa, S. (1997). Molecular genetic analysis of synaptic plasticity, activity-dependent neural development, learning and memory in the mammalian brain. Annu. Rev. Neurosci. *20*, 157–184.

Chen, C., Kano, M., Chen, L., Bao, S., Kim, J.J., Hashimoto, K., Thompson, R.F., and Tonegawa, S. (1995). Impaired motor coordination correlates with persistent multiple climbing fiber innervation in PKCγ mutant mice. Cell *83*, 1233–1242.

Conquet, F., Bashir, Z.I., Davies, C.H., Daniel, H., Ferraguti, F., Bordi, F., Franz-Bacon, K., Reggian, A., Matarerse, V., Conde, F., et al. (1994). Motor deficit and impairment of synaptic plasticity in mice lacking mGluR1. Nature *372*, 237–242.

Crépel, F., and Mariani, J. (1976). Multiple innervation of Purkinje cells by climbing fibers in the cerebellum of the weaver mutant mouse. J. Neurobiol. *7*, 579–582.

Crépel, F., Delhaye-Bouchaud, N., Guastavina, J.M., and Sampaio,

I. (1980). Multiple innervation of cerebellar Purkinje cells by climbing fibers in staggerer mutant mouse. Nature *283*, 483–484.

De Schutter, E. (1995). Cerebellar long-term depression might normalize excitation of Purkinje cells: a hypothesis. Trends Neurosci. *18*, 291–295.

De Schutter, E. (1997). A new functional role for cerebellar long-term depression. The Cerebellum: from Structure to Control, De Zeeuw, Strata, and Voogd, eds. Prog. Brain Res. *114*, 529–542.

De Zeeuw, C.I., Holstege, J.C., Ruigrok, T.J., and Voogd, J. (1989). Ultrastructural study of the GABAergic, cerebellar, and mesodiencephalic innervation of the cat medial accessory olive: anterograde tracing combined with immunocytochemistry. J. Comp. Neurol. *284*, 12–35.

De Zeeuw, C.I., Wylie, D.R., DiGiorgi, P.L., and Simpson, J.I. (1994). Projections of individual Purkinje cells of identified zones in the flocculus to the vestibular and cerebellar nuclei in the rabbit. J Comp. Neurol. *349*, 428–447.

De Zeeuw, C.I., Wylie, D.R., Stahl, J.S., and Simpson, J.I. (1995). Phase relations of Purkinje cells in the rabbit flocculus during compensatory eye movements. J. Neurophysiol. *74*, 2051–2063.

De Zeeuw, C.I., Koekkoek, S.K.E., Wylie, D.R.W., and Simpson, J.I. (1997). Association between dendritic lamellar bodies and complex spike synchrony in the olivocerebellar system. J. Neurophysiol. *77*, 1747–1758.

Doerner, D., Pitler, T.A., and Alger, B.E. (1988). Protein kinase C activators block specific calcium and potassium current components in isolated hippocampal neurons. J. Neurosci. *8*, 4069–4078.

Ekerot, C.-F., and Kano, M. (1985). Long-term depression of parallel fibre synapses following stimulation of climbing fibres. Brain Res. *342*, 357–360.

Farley, J., and Auerbach, S. (1986). Protein kinase C activation induces conductance changes in *Hermissenda* photoreceptors like those seen in associative learning. Nature *319*, 220–223.

Funabiki, K., Mishina, M., and Hirano, T. (1995). Retarded vestibular compensation in mutant mice deficient in δ2 glutamate receptor subunit. Neuroreport *7*, 189–192.

Garcia, M.M., and Harlan, R.E. (1997). Protein kinase C in central vestibular, cerebellar, and precerebellar pathways of the rat. J. Comp. Neurol. *385*, 26–42.

Grega, D.S., Werz, M.A., Macdonald, R.L. (1987). Forskolin and phorbol esters reduce the same potassium conductance of mouse neurons in culture. Science *235*, 345–348.

Hartell, N.A. (1996). Strong activation of parallel fibers produces localized calcium transients and a form of LTD that spreads to distant synapses. Neuron *16*, 601–610.

Highstein, S.M., Partsalis, A., and Arikan, R. (1997). Role of the Y-group of the vestibular nuclei and flocculus of the cerebellum in motor learning of the vestibulo-ocular reflex. The Cerebellum: from Structure to Control, De Zeeuw, Strata, and Voogd, eds. Prog. Brain Res. *114*, 383–401.

House, C., and Kemp, B.E. (1987). Protein kinase C contains a pseudosubstrate prototope in its regulatory domain. Science *238*, 1726–1728.

Huang, F.L., Yoshida, Y., Nakabayashi, H., Friedman, D.P., Ungerleider, L.G., Young, W.S., III., and Huang, K.P. (1989). Type I protein kinase C isozyme in the visual-information-processing pathway of monkey brain. J. Cell. Biochem. *39*, 401–410.

Huang, F.L., Young, W.S., III., Yoshida, Y., and Huang, K.P. (1990). Developmental expression of protein kinase C isozymes in rat cerebellum. Dev. Brain Res. *52*, 121–130.

Hummler, E., Cole, T.J., Blendy, J.A., Ganss, R., Aguzzi, A., Schmid, W., Beermann, F., and Schutz, G. (1994). Targeted mutation of the CREB gene: compensation within the CREB/ATF family of transcription factors. Proc. Natl. Acad. Sci. USA. *91*, 5647–5651.

Ito, M. (1982). Cerebellar control of the vestibulo-ocular reflex—around the flocculus hypothesis. Annu. Rev. Neurosci. *5*, 275–296.

Ito, M. (1989). Long-term depression. Annu. Rev. Neurosci. *12*, 85–102.

Ito, M., Jastreboff, P.J., and Miyashita, Y. (1982). Specific effects of unilateral lesions in the flocculus upon eye movements in albino rabbits. Exp. Brain Res. *45*, 233–242.

Jande, S.S., Maler, L., and Lawson, D.E.M. (1981). Immunohistochemical mapping of vitamin D-dependent calcium-binding protein in brain. Nature *294*, 765–767.

Kano, M., Hashimoto, K., Chen, C., Abeliovich, A., Aiba, A., Kurihara, H., Watanabe, M., Inoue, Y.L., and Tonegawa, S. (1995). Impaired synapse elimination during cerebellar development in PKCγ mutant mice. Cell *83*, 1223–1231.

Kano, M., Hashimoto, K., Kurihara, H., Watanabe, M., Inoue, Y., Aiba, A., and Tonegawa, S. (1997). Persistent multiple climbing fiber innervation of cerebellar Purkinje cells in mice lacking mGluR1. Neuron *18*, 71–79.

Kashiwabuchi, N., Ikeda, K., Araki, K., Hirano, T., Shibuki, K., Takayama, C., Inoue, Y., Kutsuwada, T., Yagi, T., Kang, et al. (1995). Impairment of motor coordination, Purkinje cell synapse formation, and cerebellar long-term depression in GluRd2 mutant mice. Cell *81*, 245–252.

Khater, T.T., Quinn, K.J., Pena, J., Baker, J.F., and Peterson, B.W. (1993). The latency of the cat vestibulo-ocular reflex before and after short- and long-term adaptation. Exp. Brain Res. *94*, 16–32.

Koekkoek, S.K.E., Alphen, A.M.V., Galjart, N., Burg, J.V.D., Grosveld, F., and De Zeeuw, C.I., (1997). Gain adaptation and phase dynamics of compensatory eye movements in mice. Genes Function *1*, 175–190.

Konnerth, A., Dreessen, J., and Augustine, G.J. (1992). Brief dendritic calcium signals initiate long-lasting synaptic depression in cerebellar Purkinje cells. Proc. Natl. Acad. Sci. USA *89*, 7051–7055.

Leclerc, N., Schwarting, G.A., Herrup, K., Hawkes, R., and Yamamoto, M. (1992). Compartmentation in mammalian cerebellum: Zebrin II and P-path antibodies define three classes of sagittally organized bands of Purkinje cells. Proc. Natl. Acad. Sci. USA *89*, 5006–5010.

Lev-Ram, V., Jiang, T., Wood, J., Lawrence, D.S., and Tsien, R.Y. (1997). Synergies and coincidence requirements between NO, cGMP, and Ca^{2+} in the induction of cerebellar long-term depression. Neuron *18*, 1025–1038.

Linden, D.J. (1994). Input-specific induction of cerebellar long-term depression does not require presynaptic alteration. Learn. Mem. *1*, 121–128.

Linden, D.J. (1996). Cerebellar long-term depression as investigated in a cell culture preparation. Behav. Brain Sci. *19*, 339–346 and 482–487.

Linden, D.J., and Connor, J.A. (1991). Participation of postsynaptic PKC in cerebellar long-term depression in culture. Science *254*, 1656–1659.

Linden, D.J., and Connor, J.A. (1995). Long-term synaptic depression. Annu. Rev. Neurosci. *18*, 319–357.

Linden, D.J., Dickinson, M.H., Smeyne, M., and Connor, J.A. (1991). A long-term depression of AMPA currents in cultured cerebellar Purkinje neurons. Neuron *7*, 81–89.

Linden, D.J., Smeyne, M., Sun, S.C., and Connor, J.A. (1992). An electrophysiological correlate of protein kinase C isozyme distribution in cultured cerebellar neurons. J. Neurosci. *12*, 3601–3608.

Linden, D.J., Dawson, T.M., and Dawson, V.L. (1995). An evaluation of the nitric oxide/cGMP/cGMP-dependent protein kinase cascade in the induction of cerebellar long-term depression in culture. J. Neurosci. *15*, 5098–5105.

Lisberger, S.G. (1988). The neural basis for learning of simple motor skills. Science *242*, 728–735.

Lisberger, S.G. (1994). Neural basis for motor learning in the vestibulo-ocular reflex of primates. III. Computational and behavioral analysis of the sites of learning. J. Neurophysiol. *72*, 974–998.

Lisberger, S.G., Miles, F.A., and Optican, L.M. (1983). Frequency-selective adaptation: evidence for channels in the vestibulo-ocular reflex? J. Neurosci. *3*, 1234–1244.

Llinás, R., Lang, E.J., and Welsh, J.P. (1997). The cerebellum, LTD, and memory: alternative views. Learn. Mem. *3*, 445–455.

Lomeli, H., Sprengel, R., Laurie, D.J., Kohr, G., Herb, A., Seeburg,

P., Wisden, W. (1993). The rat delta-1 and delta-2 subunits extend the excitatory amino acid receptor family. FEBS Lett. *315*, 318–322.

Mariani, J., Crépel, F., Mikoshiba, K., Changeux, J.P., and Sotelo, C. (1977). Anatomical, physiological, and biochemical studies of the cerebellum from reeler mutant mouse. Phil. Trans. R. Soc. (Lond.) *281*, 1–28.

Mayford, M., Bach, M.E., Huang, Y.-Y., Wang, L., Hawkins, R.D., and Kandel, E.R. (1996). Control of memory formation through regulated expression of a CaMKII transgene. Science *274*, 1678–1683.

Merchenthaler, I., Liposits, Z., Reid, J.J., and Wetsel, W.C. (1993). Light and electron microscopic immunocytochemical localization of PKCδ immunoreactivity in the rat central nervous system. J. Comp. Neurol. *336*, 378–399.

Nagao, S. (1983). Effects of vestibulocerebellar lesions upon dynamic characteristics and adaptation of vestibulo-ocular and optokinetic responses in pigmented rabbits. Exp. Brain Res. *53*, 36–46.

Narasimhan, K., and Linden, D.J. (1996). Defining a minimal computational unit for cerebellar long-term depression. Neuron *17*, 333–341.

Newton, A.C. (1995). Protein kinase C: structure, function, and regulation: a minireview. J. Biol. Chem. *270*, 28495–28498.

Oberdick, J., Levinthal, F., and Levinthal, C. (1988). A Purkinje cell differentiation marker shows a partial sequence homology to the cellular sis/PDGF2 gene. Neuron *1*, 367–376.

Oberdick, J., Smeyne, R.J., Mann, J.R., Zackson, S., and Morgan, J.I. (1990). A promoter that drives transgene expression in cerebellar Purkinje and retinal bipolar neurons. Science *248*, 223–226.

Oberdick, J., Schilling, K., Smeyne, R.J., Corbin, J.G., Bocchiaro, C., and Morgan, J.I. (1993). Control of segment-like patterns of gene expression in the mouse cerebellum. Neuron *10*, 1007–1018.

Pastor, A.M., de la Cruz, R.R., and Baker, R. (1994). Cerebellar role in adaptation of the goldfish vestibuloocular reflex. J. Neurophysiol. *72*, 1383–1394.

Powell, K.D., Quinn, K.J., Rude, S.A., Peterson, B.W., and Baker, J.F. (1991). Frequency dependence of cat vestibulo-ocular reflex direction adaptation: single frequency and multifrequency rotations. Brain Res. *550*, 137–141.

Raymond, J.L., Lisberger, S.G., and Mauk, M.D. (1996). The cerebellum: a neuronal learning machine? Science *272*, 1126–1131.

Robinson, D.A. (1976). Adaptive gain control of vestibuloocular reflex by the cerebellum. J. Neurophysiol. *39*, 954–969.

Sakurai, M. (1990). Calcium is an intracellular mediator of the climbing fiber in induction of cerebellar long-term depression. Proc. Natl. Acad. Sci. USA *87*, 3383–3385.

Schilling, K., Dickinson, M., Connor, J.A., and Morgan, J.I. (1991). Electrical activity in cerebellar cultures determines Purkinje cell dendritic growth patterns. Neuron *7*, 891–902.

Schilling, K., Schmidt, H.H.H.W., and Baader, S.L. (1994). Nitric oxide synthase expression reveals compartments of cerebellar granule cells and suggests a role for mossy fibers in their development. Neuroscience *59*, 893–903.

Shibuki, K., Gomi, H., Chen, L., Bao, S., Kim, J.J., Wakatsuki, H., Fujisaki, T., Fujimoto, K., Katoh, A., Ikeda, T., et al. (1996). Deficient cerebellar long-term depression, impaired eyeblink conditioning, and normal motor coordination in GFAP mutant mice. Neuron *16*, 586–599.

Shigemoto, R. (1992). Distribution of the mRNA for a metabotropic glutamate receptor (mGluR1) in the central nervous system: an in situ hybridization study in adult and developing rat. J. Comp. Neurol. *322*, 121–135.

Shigemoto, R., Abe, T., Nomura, S., Nakanishi, S., and Hirano, T. (1994). Antibodies inactivating mGluR1 metabotropic glutamate receptor block long-term depression in cultured Purkinje cells. Neuron *12*, 1245–1255.

Shimohama, S., Saitoh, T., and Gage, F.H. (1990). Differential expression of protein kinase C isozymes in rat cerebellum. J. Chem. Neuroanat. *3*, 367–375.

Simpson, J.I., Wylie, D.R., and De Zeeuw, C.I. (1996). On climbing fiber signals and their consequence(s). Behav. Brain Sci. *19*, 380–394.

Smeyne, R.J., Chu, T., Lewin, A., Bian, F., Sanlioglu, S., Kunsch, C., and Oberdick, J. (1995). Local control of granule cell generation by cerebellar Purkinje cells. Mol. Cell. Neurosci. *6*, 230–251.

Stevens, C.F. (1996). Spatial learning and memory: the beginning of a dream. Cell *87*, 1147–1148.

Thompson, R.F., and Krupa, D.J. (1994). Organization of memory traces in the mammalian brain. Annu. Rev. Neurosci. *108*, 44–56.

Tsien, J.Z., Huerta, P.T., and Tonegawa, S. (1996a). The essential role of hippocampal CA1 NMDA receptor-dependent synaptic plasticity in spatial memory. Cell *87*, 1327–1338.

Tsien, J.Z., Chen, D.F., Gerber, D., Tom, C., Mercer, E.H., Anderson, D. J., Mayford, M., Kandel, E.R., and Tonegawa, S. (1996b). Subregion- and cell type-restricted gene knockout in mouse brain. Cell *87*, 1317–1326.

Voogd, J., and Bigaré, F. (1980). Topographical distribution of olivary and cortico nuclear fibers in the cerebellum: a review. In The Inferior Olivary Nucleus: Anatomy and Physiology, J. Courville, ed. (New York: Raven Press), pp. 207–235.

Wetsel, W.C., Khan, W.A., Merchenthaler, I., Rivera, H., Halpern, A.E., Phung, H.M., Nego-Vilar, A., and Hannun, Y.A. (1992). Tissue and cellular distribution of the extended family of protein kinase C isozymes. J. Cell Biol. *117*, 121–133.

Yeo, C.H., Hardiman, M.J., and Glickstein, M. (1985). Classical conditioning of the nictitating membrane response of the rabbit: 1. lesions of the cerebellar nuclei. Exp. Brain Res. *60*, 87–98.

Yoshida, Y., Huang, F.L., Nakabayashi, H., and Huang, K.P. (1988). Tissue distribution and developmental expression of protein kinase C isozymes. J. Biochem. Chem. *20*, 9868–9873.

Young, W.S., III. (1988). Expression of three (and a putative four) protein kinase C genes in brains of rat and rabbit. J. Chem. Neuroanat. *1*, 177–194.

Zee, D.S., Yamazaki, A., Butler, P.H., and Gucer, G. (1981). Effects of ablation of flocculus and paraflocculus of eye movements in primate. J. Neurophysiol. *46*, 878–899.